2

High Density Devices Applied to a Gamma-Camera Implementation

Griselda Saldana-Gonzalez[1], Uvaldo Reyes[2], Humberto Salazar[2], Oscar Martínez[2], Eduardo Moreno[2] and Ruben Conde[2]
[1]*Electric and Electronics Department, Universidad Tecnologica de Puebla*
[2]*Physics and Mathematics Faculty, Benemerita Universidad Autonoma de Puebla*
Mexico

1. Introduction

Image processing is considered to be one of the most rapidly evolving areas of information technology, with growing applications in all fields of knowledge. It constitutes a core area of research within the computer science and engineering disciplines given the interest of potential applications ranging from image enhancing, to automatic image understanding, robotics and computer vision. The performance requirements of image processing applications have continuously increased the demands on computing power, especially when there are real time constraints. Image processing applications may consist of several low level algorithms applied in a processing chain to a stream of input images. In order to accelerate image processing, there are different alternatives ranging from parallel computers to specialized ASIC architectures. The computing paradigm using reconfigurable architectures based on Field Programmable Gate Arrays (FPGAs) promises an intermediate trade-off between flexibility and performance.

In the present work a prototype for reconstruction of two-dimensional images based in FPGAs is presented. The front-end includes two main modules, the data acquisition electronics and a hardware architecture for data processing. The read out electronics consists mainly of a Discretized Positioning Circuit (DPC), analog-to-digital converters and a FPGA Virtex IV of the Xilinx's family. This module reads the electrical signals produced by a Position-Sensitive Photomultiplier Tube (PS-PMT) coupled to a Cerium-doped Lutetium Yttrium Orthosilicate (LYSO) crystal. The hardware architecture takes the digitized signals produced by the acquisition module and processes them to determine the positions of the interactions based on the logic of Anger to form a planar image. The architecture performs arithmetic operations, formats the data and stores them in memory blocks to be sent to the displaying stage. The final image obtained represents a 2D histogram for the intensity distribution of the radioactivity. Both systems interact to operate at a clock frequency of 322 MHz reducing the processing time to reach real time performance. Using parallelism techniques and an appropriate management of memory, the necessary logic to implement the system has been developed improving flexibility for adjustment to new requirements or new algorithms. The main contribution of this work consists on validating the use of FPGAs in the image processing stage in a nuclear medicine application, such as gamma camera.

This chapter shows a brief introduction to the physics involved in the operation of a gamma camera. Some details regarding the characteristics of the sensors used to obtain signals and the mechanism to interpret them and to relate them with the formation of a gammagram are presented. Details of the acquisition systems and image formation architecture proposed are explained. The obtained results are shown highlighting the benefits that can be provided by a system implemented with FPGA technology and reconfigurable computing. Finally some conclusions are presented.

2. Physics of the gamma camera

The discovery of radioactivity and the natural radioactive elements at the end of the last century marked the beginning of a series of important discoveries that completely changed the idea of the matter structure. This allowed the use of radiation for medical applications and in other areas.

Nuclear Medicine is based on the detection of nuclear radiation emitted by a human body after inserting a radiopharmaceutical. Although its birth has not an exact date, it begins with the discovery of polonium by Pierre Curie and Marja Sklodowska-Curie in 1898, however, the concept of producing images for diagnosis using radioactive materials is more recent. The first medical report on the use of a radioactive substance was made by Eugene Bloch and the French physicist Henri Danlos when they placed radio in contact with a skin lesion caused by tuberculosis.

One of the most significant developments in image instrumentation was the scintillation camera developed by Anger in 1952 (Anger, 1958). This camera is also known as gamma camera or Anger camera, it is of great use in nuclear medicine due to it allows to obtain useful medical images called gammagram (see Fig. 1).

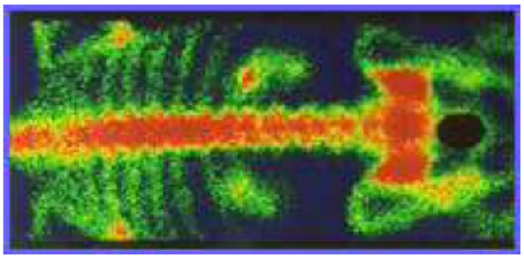

Fig. 1. Gammagram. Hot areas are marked in red; they indicate a higher radiopharmaceutical concentration. Cold areas have a less concentration

Nuclear medicine, as diagnostic method, highlights biochemical and functional processes for a particular organ or tissue; radioactive elements emitting photons or positrons joined to drugs are used. The amount of radiation emitted from the host tissue describes its metabolism.

Unlike x-ray diagnosis, which uses an x-ray emitting source, from where a percentage interacts with the patient and the resulting beam is analyzed on a detector film, in the gamma camera diagnosis, the patient is the radioactive emitter source of gamma photon and using the appropriate detector certain information from the target tissue is obtained.

2.1 The energy of radiation

In general, radioactive elements are those which have an excess of protons or neutrons. When the number of neutrons equals the number of protons is more difficult that the strong nuclear force hold them together. Eventually, the imbalance is corrected by release of excess neutrons or protons in the form of α particles (*He* nucleus) and particles that can be electrons or positrons.

These emissions lead to two types of radiation:

- α radiation, which lightens the atomic nucleus by four mass units and changes the atomic number two units.
- β radiation, which does not change the mass of the nucleus as it involves the conversion of a proton into a neutron or vice versa and change the atomic number in a single unit (positive or negative, depending on the emitted particle, either an electron or a positron).

There is also a third type of radiation in which high-frequency photons called γ radiation are emitted. This type of radiation is due to the nucleus passes from an excited state of higher energy to a lower energy state. γ radiation is a very penetrating electromagnetic radiation because the photons have no electrical charge.

In the case of protons, electrons, neutrons, α particles, heavy ions, etc., the E energy is the kinetic energy given by the classical equation:

$$E = \frac{1}{2}mv^2 \tag{1}$$

Where m is the mass and v the particle speed. The Joule, J, is the energy unit in the international system.

On the other hand, radiations provide a vehicle for transporting energy from one place (the source) to another (the absorber). The electron volt [eV] is the unit used in radiation physics and it is defined as the energy acquired by a particle with electric charge e (electron electric charge of 1.6×10^{-19} C) in a potential difference of 1 Volt. The equivalence with the Joule is $1eV=1.60\times10^{-19}$ J.

Since light has wave-particle duality, at times it behaves as particle and some other shows wave characteristics. Thus, a photon has an energy given by:

$$E = hv \tag{2}$$

Where h is the Planck constant (equal to 6.626×10^{-34} Js) and v is the wave frequency.

Photons travel at the speed of light in vacuum c, as:

$$v = \frac{c}{\lambda} \tag{3}$$

Where λ is the wavelength.

One result of the relativity theory is the possibility of converting mass into energy and vice versa obeying the formula:

$$E = mc^2 \tag{4}$$

2.2 Radiation sources

In this work the referred radiation is the one caused by jumps of electrons around the nucleus, which is called X-rays, but mainly to the radiation originated from transitions within the nucleus, gamma rays.

Most sources used for radiation measuring are radioisotopes that decay by emission of a beta-less. This process can be described as follows:

$$ {}^{A}_{Z}X \rightarrow {}_{Z+1}{}^{A}Y + \beta^{-} + \bar{\nu} \tag{5} $$

Where X and Y are the nucleus of the initial and final elements, and $\bar{\nu}$ is an antineutrino. The nucleus of the initial element is called the father nucleus and the nucleus of the final element is called a son nucleus. Due to neutrinos and antineutrinos have a low probability of interaction with matter, they are virtually undetectable, and thus ionizing radiation produced by beta decay is the fast electron or beta particle.

After a beta less decay the nucleus is in a metastable state and to reach its base state it emits a gamma photon. As the nuclear states have well defined energies, the gamma ray energy emitted in the transition from state to state is also well defined.

All the above processes can be displayed in a decay scheme as shown in Fig. 2, where a horizontal line represents the father nucleus, and the final horizontal line represents the son nucleus. The horizontal lines between these two lines represent intermediate excited states. A diagonal line to the left shows an electron capture decay, a small vertical line followed by a diagonal line to the left indicates a β^{+} or alfa decay, and a right diagonal line indicates a β^{-} decay. Vertical lines indicate the emission of gamma rays.

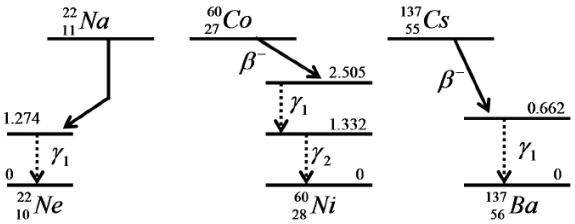

Fig. 2. To the left is the decay scheme of ^{22}Na. At the center is the decay scheme of ^{60}Co. To the right is the decay scheme of ^{137}Cs

In order to calibrate the systems, four sources of radiation: ^{22}Na, ^{57}Co, ^{60}Co and ^{137}Cs are commonly used. Their decay schemes are shown in Fig. 2. The ^{22}Na decays by the process of β^{+} emitting a gamma photon of 1.274 MeV when the nucleus is stable, but also emits two gamma photons of 511 keV product of the annihilation of positron. The ^{60}Co decays to ^{60}Ni via a β^{-}, it emits two photons of 1.173 and 1.332 MeV. ^{137}Cs decays to ^{137}Ba also by a β^{-} process, 6.5% of the time decays directly to ^{137}Ba and 93.5% decays to ^{137}mBa emitting a gamma photon of 662 keV, 85% of the times.

Reference sources are an essential accessory to measure radiation in a laboratory. Usually, they are samples of radioisotopes of few microcuries encapsulated in plastic disc. The

thickness of the package is enough to stop the radiation from the father nucleus decay allowing the passage only to the gamma radiation produced by the decay of the son nucleus.

2.3 Photon-matter interaction

When X-rays or gamma rays pass through a medium, the interaction between photons and matter can be noticed by the result of energy transferred to the medium. Due to the abundance of electrons in any substance, the most common interaction process of different radiations is with the electrons in the material, giving rise to the ionization and excitation phenomena. Through these processes, radiations usually deposit almost all their energy on the substances with which they collide. A high percentage of this energy ends up as heat, raising the temperature of the material, but part of the energy deposited can also cause chemical reactions and changes in the material structure.

The attenuation of a photons beam by an absorber material is mainly caused by four types of interactions: coherent scattering, photoelectric effect, Compton effect and pair production. Each of these processes can be represented by its own coefficient of attenuation, which varies according to the incident photon energy and atomic number of absorber material.

2.3.1 Coherent scattering

Coherent scattering is also known as classic scattering or Rayleigh scattering. This interaction consists of an electromagnetic wave that passes near an electron and makes it oscillate. The oscillating electron re-radiates energy at the same frequency as the incident electromagnetic wave. In this way, there is no change in energy and there is not absorbed energy by the medium, there is only a photon scattering effect for small angles. The coherent scattering is probable for materials with high atomic numbers and low energy photons.

2.3.2 Photoelectric effect

The photoelectric effect is a phenomenon in which a photon interacts with an atom and ejects an orbiting electron as shown in Fig. 3. In this process the photon's energy $h\upsilon$ is absorbed by the atom and then it is transferred to the electron. The kinetic energy of the ejected electron (called a *photoelectron*) is equal to $h\upsilon - E_B$, where E_B is the binding energy of the electron. Interactions of this kind can take place with electrons in layers *K*, *L*, *M* or *N*.

After that the electron has been ejected from the atom, a hole is created in this orbital; with this the atom is in an excited state. The hole can be filled by another electron from the external orbital, emitting radiation known as X-ray.

2.3.3 Compton effect

The Compton effect is a logical extension of the photoelectric effect. The difference is that in this case the photons are generally more energetic than when the photoelectric effect occurs (X-rays or gamma rays) and as a result, all its energy is not used to remove and accelerate an electron. In this case, there is excess energy and the photon does not disappear completely.

In this interaction the incident photon with energy E_0 and an associated wavelength, λ_0, from Equation (2), interacts with an electron that is free in the material, Fig. 3. The result is a low energy photon E_λ and an electron that goes back with a kinetic energy T depending on the angle of the leaving new photon.

It is common that the Compton effect occurs when the incident photons falls within a range from 0.05 MeV to several MeV. The energy range overlaps with the photoelectric energy range. With very low photon energies, the photoelectric effect is dominant, but becomes less common with increasing photon energy. The Compton effect begins slowly at low levels of energy and becomes dominant from 0.1 to 0.15 MeV and onwards, see Fig. 4.

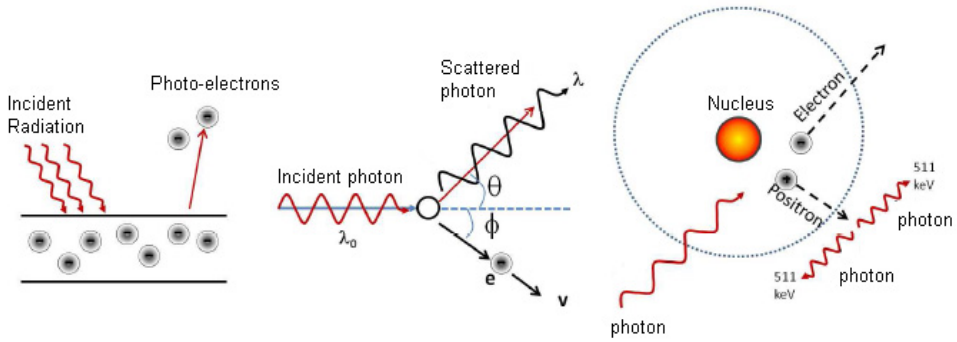

(a) Photoelectric effect (b) Compton effect (c) Pairs production

Fig. 3. In photoelectric effect, a material emits electrons when electromagnetic radiation incides on it. In Compton effect, the electromagnetic radiation striking out a surfaces goes out with a wavelength greater than the input. In pair production a photon interacts with a nucleus, completely disappears and results in the creation of a particle-antiparticle pair, electron-positron

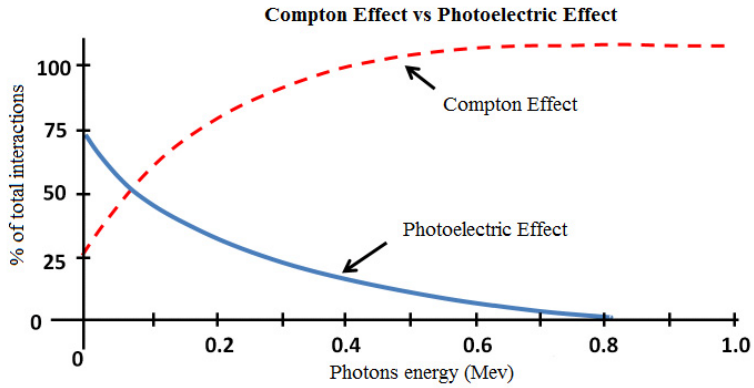

Fig. 4. With very low photon energies, the photoelectric effect is dominant. The Compton effect becomes dominant from 0.1 to 0.15 MeV and onwards

2.3.4 Pairs production

In this process the photon full energy is converted within an atom in a positron-electron pair, Fig. 3. As in the photoelectric effect, pairs production requires the presence of a body with large *Z*. Furthermore, in this process the photon must have energy greater than or equal to 1.022 MeV.

2.4 Ionizing radiation detection

Since the ionizing radiation is generally not perceptible by the senses, it is necessary to use appropriate tools to detect its presence. Many types of radiation detectors have been developed and each one is sensitive to certain types of radiation and energy range, therefore it is essential to select the appropriate detector for the radiation to be measured.

Radiation detectors have been developed based on the interactions of ionizing radiation with matter described above. The idea is to measure the lost energy or deposited by radiation when passing through the detector. Radiation detectors convert the energy deposited in a measurable electrical signal of few volts, which is achieved by constructing a diagram called characteristic energy spectrum (see Fig. 5). If there is mono-energetic radiation incident, variations in the measurements of that energy would appear due to an incomplete deposit of the incident radiation. For example, in a gamma camera some of the incident photons of 82 keV can have one or more Compton scatterings depositing part of their energy and then leave the detector.

The continuous proportion in the energy spectrum shown in Fig. 5 is due to partial energy deposits. The peak position marks the average energy of the incident radiation (after a full deposit in the detector).

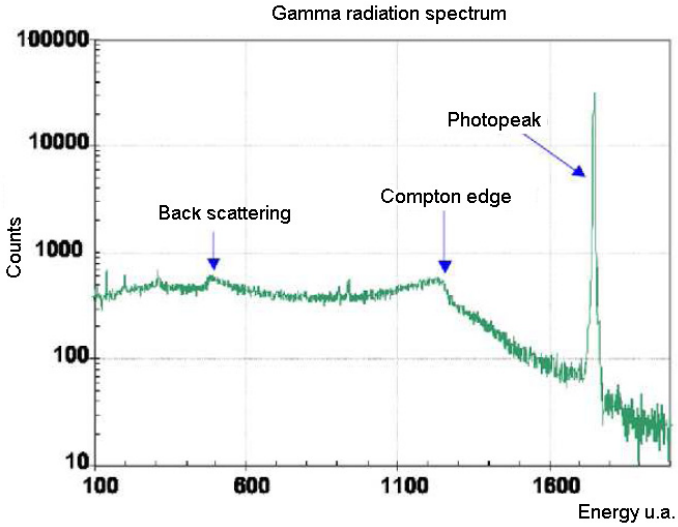

Fig. 5. Typical spectrum of gamma radiation, where the photopeak, the Compton edge and the backscattering peak are shown

The width of this peak (called photopeak) shows the effect of fluctuations for energy deposits for a mono-energetic photon. The detector's ability to accurately measure the energy deposited is an important parameter and is characterized by the width of the photopeak in the energy spectrum, referred to as the energy resolution of the system.

Radiation detectors generally used in the mini gamma cameras are called scintillation detectors. They are composed of an inorganic crystal (scintillator) and a photodetector. The scintillator crystal emits photons with wavelengths in the visible after radiation-matter interaction occurs inside the crystal. The photodetector is used to detect and measure the number of photons emitted by an interaction in the scintillator crystal. The number of photons due to scintillation (or intensity) is generally proportional to the energy deposited within the crystal. Due to the high atomic number, and therefore high density, scintillator detectors give high braking efficiency for photons of about 500 keV.

3. The mini gamma camera

The mini gamma camera is an imaging device commonly used in nuclear medicine as a diagnostic tool. The radiation comes from the patient who is previously injected, usually intravenously, with a radioactive tracer. The mode of conducting the clinical diagnosis is called scintigraphy.

The radioisotope tracer can be monitored inside the patient's body by the mini gamma camera and making easier to establish a medical diagnosis. The analysis offered by the gammagrams is especially functional rather than anatomical such as x-rays. They serve to assess whether a patient's metabolism is working properly adhering tracers, for example in platelets, red blood cells or other cells where a correct operation is checked. It is possible to mark the glucose molecules to assess which areas of the brain are activated (consume more glucose) at certain times.

Without loss of generality it can be say that a gamma camera consists of three components: a head or radiation detector, a data acquisition system and image reconstruction algorithms, as shown in Fig. 6.

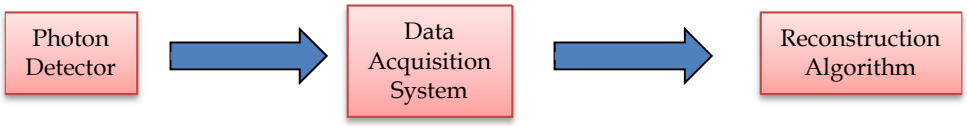

Fig. 6. Schematic of the gamma camera parts. The three components are: a head or radiation detector, an electronic data acquisition system and image reconstruction algorithms

The photon detector is responsible for converting the radiation-matter interaction into analog electrical pulses; it is usually composed of a collimator, a scintillator crystal and a photomultiplier tube (PMT). The collimator allows the passage only of radiation emitted perpendicular to the head and is usually constructed of lead or tungsten. In the scintillator crystal take place radiation-matter interaction processes between photons and the material that constitute the scintillator crystal, usually sodium iodide, $NaI(Tl)$ or Cesium Iodide, $CsI(Tl)$, both activated with thallium, to deliver lower energy photons (ultraviolet radiation).

The PMT is able to detect ultraviolet photons and turn them into a measurable electrical pulse in order to be processed by the appropriate electronics.

3.1 Photon detector

A radiation detector is a device used to track and identify high-energy particles, such as those produced by radioactive decay, cosmic radiation or reactions in a particle accelerator. In nuclear physics, radiation detectors capable of identifying energies in the order of keV are used.

The photon detector for the mini gamma camera consists of a collimator, a scintillator crystal, an array of photomultiplier tubes and positioning electronics.

3.2 Collimator

Leaning on the detector is the collimator; it is an element that is chosen according to the needs of study (Simon et al., 2003). It is made of lead or tungsten and is crossed by a distributed set of holes with different geometric patterns. The lead bricks between the holes are called *septas*. The collimator improves the system detection.

3.3 Scintillator crystal

In high-resolution mini gamma camera or micro PET equipment, the scintillator crystals can be cut into small blocks that are grouped into a matrix, separated by a reflective material. This configuration of segmented crystals (also known as pixilated crystals) is the dominant commercial high-resolution equipment and it is intended that each crystal behaves as a small waveguide for optical photons, in order to avoid that the light produced in the interaction of gamma rays is spread.

The materials most commonly used in the mini gamma cameras have been the sodium iodide activated with thallium (*NaI:Tl*) (Sánchez et al., 2004), bigermanate of bismuth (*BGO*) (Zhang et al., 2002), the oxi-ortosilicato of gadolinium (*GSO*), oxi-ortosilicato of lutetium (*LSO*) (Demetri & Jonathon, 2005) and its variants, the last two, doped with cerium. The most interesting features of these crystals and other novel materials are shown in Table 1.

3.4 Photomultiplier tube

The photomultiplier tubes used in mini gamma cameras are sensitive to the position (PSPMT). The first requirement in this design is the use of an electron multiplier structure which maintains a spatial separation between the electrons clouds multiplied (from the photoelectrons generated in different positions on the photocathode). One of the electron multiplier structures is the metal channel dynodes.

In the structure of metal channel dynodes gives a crosstalk effect during the multiplication of secondary electrons. This is due to the emitted electrons from the photocathode go to the first dynode by the focus grille, then they flow toward the second dynode, the third, until the last dynode and finally to the anode. Fig. 7 shows this type of structure. The common method of reading the outputs of the PS-PMT is a resistive arrangement; see Fig. 8, which allows calculating the position of interaction of radiation in the scintillator crystal.

	Maximum wavelength (nm)	Refractive index	Decay Time (μs)
Alkaline			
NaI(Tl)	415	1.85	0.23
CsI(Tl)	540	1.80	0.68, 3.34
CsI(Na)	420	1.84	0.46, 4.18
slow inorganic			
BGO	480	2.15	0.30
$CdWO_4$	470	2.13	1.1, 1.45
ZnS(Ag)	450	2.36	0.2
Fast inorganic without activator			
BaF_2	220		0.0006
CsI	305		0.002, 0.02
CeF_3	310	1.68	0.005, 0.027
Cerium activated fast inorganic			
GSO	440	1.85	0.056, 0.4
YAP	370	1.95	0.027
YAG	550	1.82	0.088, 0.302
LSO	420	1.82	0.047

Table 1. Properties of some inorganic crystals

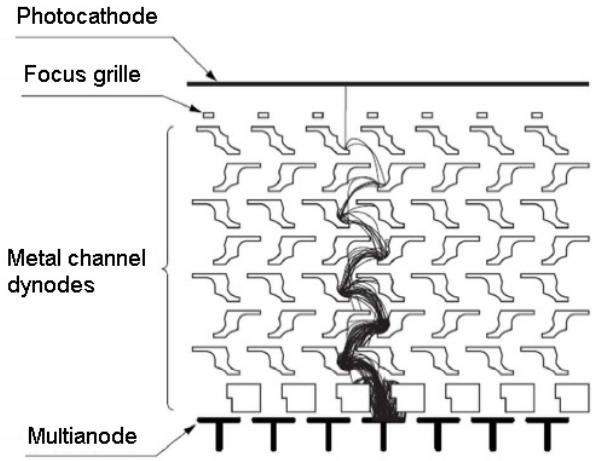

Fig. 7. Dynode structure and electrons trajectory

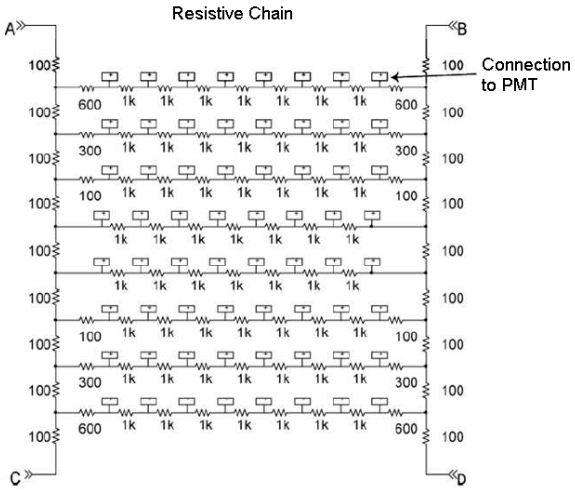

Fig. 8. Positioning circuit consisting of an array of resistors, commonly known as resistive chain

3.5 X, y positions calculation

In general to calculate an average position, the best estimate of the true value of $\vec{x}$ is given by the weighted average given by the following expression:

$$\vec{x} = \frac{\sum_i P_i \vec{x}_i}{P_i} \tag{6}$$

$\vec{x}$ indicates the position (x, y) of the event, P_i are the weights and x_i are the positions of the elements in question.

If the amount of light detected by a PMT is inversely proportional to the lateral distance between the place of interaction and the center of the PMT (Simon et al., 2003), as illustrated in Fig. 9. Ideally, the ratio between the signal amplitude in relation to the center of a PMT should be linear. In addition, the maximum measurable voltage at points A and B of the resistive chain, are also linear in relation to the center of signals delivered by the PMT. This allows calculating an event position by taking a weighted average or centroid of the PMT signals.

In this case the problem lies in knowing the position of a gamma photon interaction on the surface of the scintillator crystal. Assuming that the position of interaction is given by the values (x, y), as shown in Fig. 10, the known values are the maximum voltages (V_A, V_B, V_C and V_D) and the positions where these voltages are measured (x_1, y_2), (x_2, y_2), (x_1, y_1) and (x_2, y_1). Using equation (6) the position (x, y) is:

$$x = \frac{(V_A + V_C)x_1 + (V_B + V_D)x_2}{V_A + V_B + V_C + V_D} \tag{7}$$

$$y = \frac{(V_C + V_D)y_1 + (V_A + V_B)y_2}{V_A + V_B + V_C + V_D} \tag{8}$$

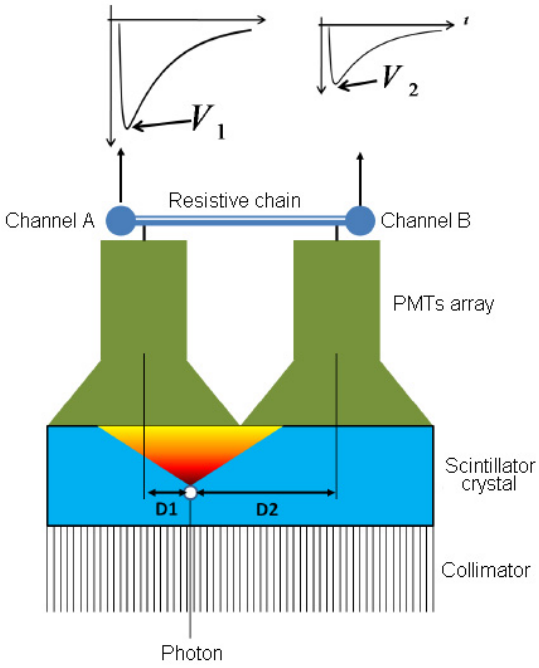

Fig. 9. Illustration of gamma radiation interacting with the photomultiplier tube

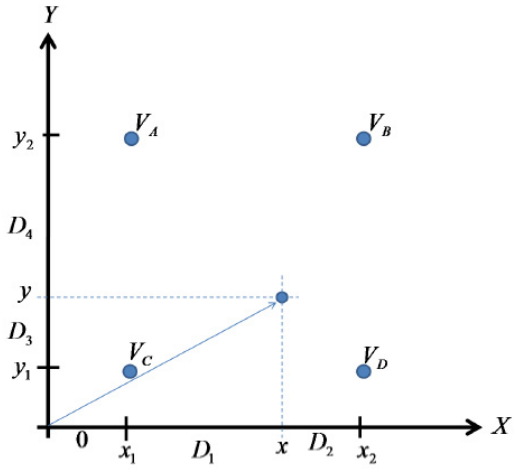

Fig. 10. Scheme to describe the process of event detection. In the Cartesian system position identifies the four voltage signals, V_A, V_B, V_C and V_D, and the position (x, y) of gamma photon interaction on the crystal

Equations (7) and (8), indicate that the sought position is a function of the maximum values, which change over time, and the known positions x_1, x_2, y_1 and y_2.

In order to remove the dependence on the known positions the following variables are defined: $D_1 = x - x_1$, $D_2 = x^2 - x$, $D_3 = y - y_1$, $D_4 = y_2 - y$, $D = D_1 + D_2$ y $D' = D_3 + D_4$, see Fig. 10. In this way, $D = x_2 - x_1$ y $D' = y_2 - y_1$, and doing simple calculations leads to the following equations:

$$x' = \frac{D_1}{D} = \frac{V_B + V_D}{V_A + V_B + V_C +} \tag{9}$$

$$y' = \frac{D_3}{D'} = \frac{V_A + V_B}{V_A + V_B + V_C + V_D} \tag{10}$$

The photon energy that interacted with the scintillator crystal is proportional to the sum of the maximum voltages:

$$E \propto V_A + V_B + V_C + V_D \tag{11}$$

As can be seen, the resistive chain helps to reduce the number of signals from the photomultiplier tubes to only four. This is not the only system to reduce the number of signals, but it is the simplest to build (Demetri, 2005).

The most important thing from equations (9), (10) and the proportionality given by (11) is that only the maximum voltage values of the four signals from the resistive chain V_A, V_B, V_C and V_D are involved. That is, it is not important to know the exact information from the whole pulse, it is enough to find its maximum value in voltage, in order to know the relative position (x, y) of the interaction on the scintillator crystal and an approximation of the energy deposited.

3.6 Data acquisition system

A data acquisition system takes analog electronic signals to generate data that can be manipulated by a computer or other electronic system (digital system). This procedure takes a set of physical signals; it turns them in current signals and digitized them in order to be processed on a computer. It is required a conditioning stage, which adapts the signal to levels compatible with the element that makes the conversion to digital. The element that makes this transformation is the digitalization module or data acquisition board. A data acquisition system is basically composed of:

- The signal sources, which are of two kinds:
  1. Direct measurement elements. They produce a signal as a result of electrical measurements, such as voltage, current, resistance, frequency, etc.
  2. Transducers. They are devices that sense physical phenomena and convert non-electrical parameters into electrical signals; examples are resistance temperature detectors, pressure transducers, among others.
- Elements of signal conditioning. These elements amplify, isolate and filter signals to make more accurate measurements.
- Data processing and display. Allows the signals visualization. Data can be displayed in analog or digital way, numerically or graphically.

3.7 Image reconstruction algorithms

The principle of image reconstruction in all forms of tomography is that an object can be reproduced exactly from a set of its projections taken from different angles. In the last two decades, several algorithms have been developed, they can be considered as methods to approximate the inverse Radon transform. They can be implemented for different tomography reconstruction modalities. It is noteworthy that these methods are not all equivalent.

3.8 Energy resolution

The energy resolution is a measure of the system's ability to distinguish between particles or photons of different energies. That can be determined by irradiating the detector with monoenergetic particles or photons and measuring the width of the Gaussian peak in the resulting heights spectrum of the acquired signals. A wider Gaussian peak implies a poorer energy resolution. The width of the Gaussian peak is usually measured at half its maximum height, as illustrated in Fig. 11, which is called *the full width at half-maximum* (FWHM). In this way the energy resolution is expressed as:

$$R = \frac{FWHM}{M} \times 100\% \tag{12}$$

R is the energy resolution and M is the energy value correspondent to the maxim Gaussian peak.

For example, the energy resolution of a crystal of 5 cm in diameter and 5 cm thick, coupled to a PMT and exposed to gamma rays of 662 keV of ^{137}Cs, is typically about 7% to 8%.

4. Materials and methods

The camera presented in this work is composed of a Hamamatsu H8500 Flat Panel PS-PMT (Hamamatsu Photonics, 2007), a LYSO scintillator (Chen, 2007), a resistive chain, a data acquisition system and a hardware architecture for image reconstruction. Fig. 12 shows a block diagram of the implemented system.

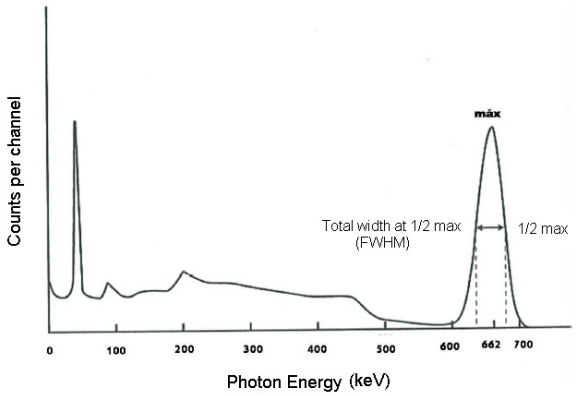

Fig. 11. Energy resolution of a height pulse spectrometer. The spectrum shown corresponds to ^{137}Cs, obtained by a scintillator *NaI* (*TI*) coupled to a photomultiplier tube.

The scintillation structure is composed of 20×20 LYSO crystal. The H8500 Flat Panel PS-PMT has an external size of 52.0×52.0×27.4 mm^3 with an active area of 49×49 mm^2; the gain of the H8500 is about 10^6 for -1000V.

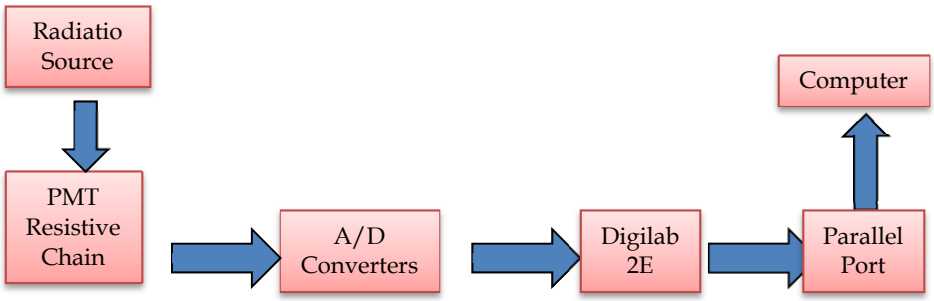

Fig. 12. Main camera connected to the data acquisition hardware

The multiplied charge is collected by an array of 8×8 anodes and the size of each anode is 5.8×5.8 mm^2. The resistive chain is composed of one board (60×60×3 mm^3) mounted orthogonally with respect to the PS-PMT according to Fig. 13 (Olcott, 2006), combined with two dedicated compact 2-channel ADC board developed in the faculty laboratory. The ADC board contains two 10 bits analogue-to-digital converters with 100 MSPS, an on-chip voltage reference of 1V to 2V p-p single-ended. The ADC boards are connected to a 2E board which allows to pick up the maximum values of the signals and stores them in a FIFO memory (data transmission is 100 MHz). The 2E board is connected to a Virtex IV based board, which allows calculating x, y position values for each event based on the Anger's logic (Equations 9, 10 and 11).

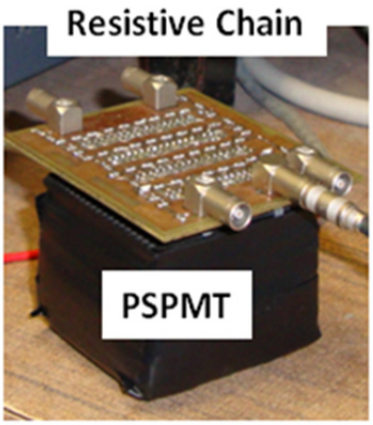

Fig. 13. Scintillator structure coupled with the resistive chain

The system allows to display planar histogram in real time mode (1s refresh time). To build a 2D image, the x and y values are used to determine a location on the image and the

brightness of the pixel at that position corresponds with the histogram value calculated (Equation 11). This process is performed until a desired number of counts on total acquisition time are reached. In order to display the results, the data are sent to a VGA monitor. The test was carried out using a ^{137}Cs point source (1microCi activity) emitting 662 keV (99%) gamma-ray lines. The architecture has been implemented using VHDL and synthesized to a XC4VFX20-FF672 Virtex IV FPGA with the Xilinx Synthesis Technology (XST) tool and placed and route with Foundation ISE 10. Inside the Virtex IV the Anger logic (Wong, 2006) is implemented profiting parallelism inherent to operation in order to achieve real time performance.

5. Results

When the acquisition system is complete, the energy spectrum of the crystal and its decay constant are obtained, the pulses shape obtained with the acquisition system for these values are presented. Finally the ^{137}Cs source is placed in a corner on the scintillator crystal and the energy resolution of the system and the first scintigraphies are obtained.

The voltage pulses registered caused by radiation from the scintillator crystal are in the range of 40 to 400 mVolts, as shown in Fig. 14. By comparing the emission spectrum of LYSO crystal is identified that he voltage range (50 to 250 mV) should match to the range of the emitted energy in the crystal, which corresponds to wavelengths from 380 to 460 nm therefore the system must be calibrated.

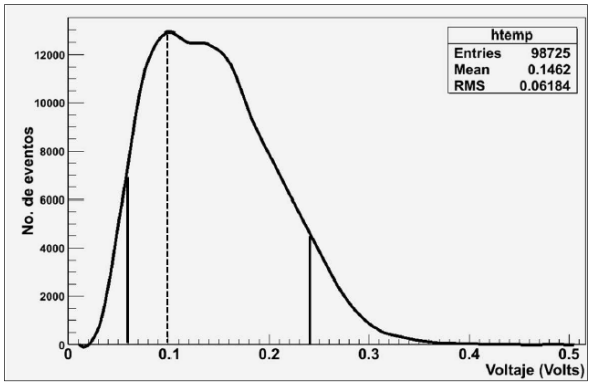

Fig. 14. Emission spectrum for the scintillator crystal

In data acquisition, 15 traces are obtained for each pulse, from these the one appearing in the fourteenth position is taken, see Fig. 14. The time in which occurs (140 ns) is known, the maximum and the trace value at 140 ns is also known. Using the following equation for different voltage pulses the histogram shown in Figure 8 is obtained.

$$\lambda = \frac{1}{t} ln \left[\frac{v(t)}{V_{max}} \right] \tag{13}$$

V_{max} is the maximum voltage, v(t) is the voltage measured at t time. The decay constant for the crystal is 41,03 ± 9,6 ns.

In order to calculate the energy resolution, first a histogram of the emission spectrum of ^{137}Cs was obtained as can be seen in Fig. 15. It is possible to identify the photopeak and using equation (12) the energy resolution is calculated.

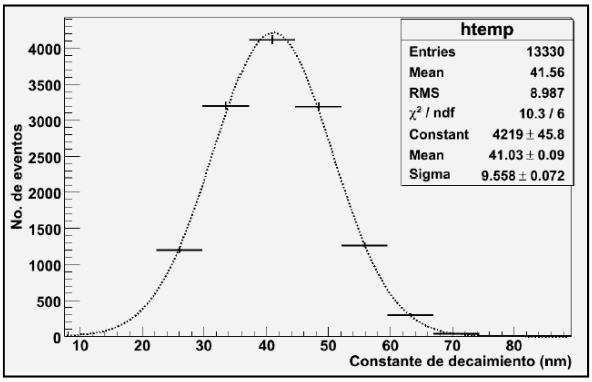

Fig. 15. Histogram to determine the decay constant of the scintillator crystal, which resulted in 41ns

The H8500 has PSPMT non-uniformity. It is known that the photomultiplier is pixilated into an array of 8×8 pixels. It is expected that each pixel has a different answer to the same power source. That is why the different responses of each pixel must be quantified and standardized with respect to the greatest response.

When the resolution of the system for all pixels is calculated, a resolution of 34% is obtained. This value is mainly affected by the PSPMT non-uniformity. For this reason the energy resolution for a single pixel was obtained, which is 19%. This result is promising because it is within the values reported in the literature (Knoll, 2000).

The image obtained with the LYSO crystal, the source of ^{137}Cs the adquisition block and the Virtex IV board can be seen in Fig. 16. The system is operating at a frequency of 322 MHz, which will give the system the capability of real time operation. The amount of area used by

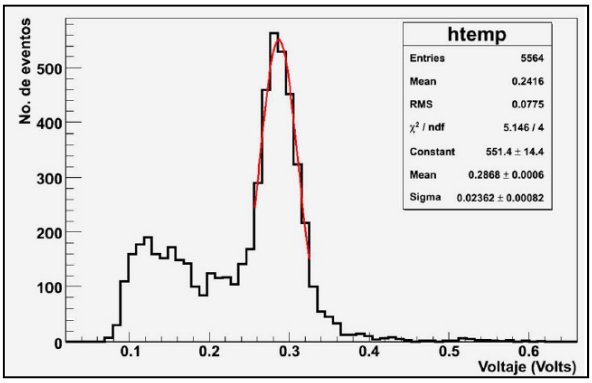

Fig. 16. Energy spectrum for the ^{137}Cs source. The value obtained was 19%

the implementation is considerably reduced, around 25% of total available in the FPGA; this is due to the implemented operations are really simple and performed in parallel. Furthermore each processing block is re-used by the data incoming to the architecture. Technical data for the FPGA architecture are resumed in Table 2.

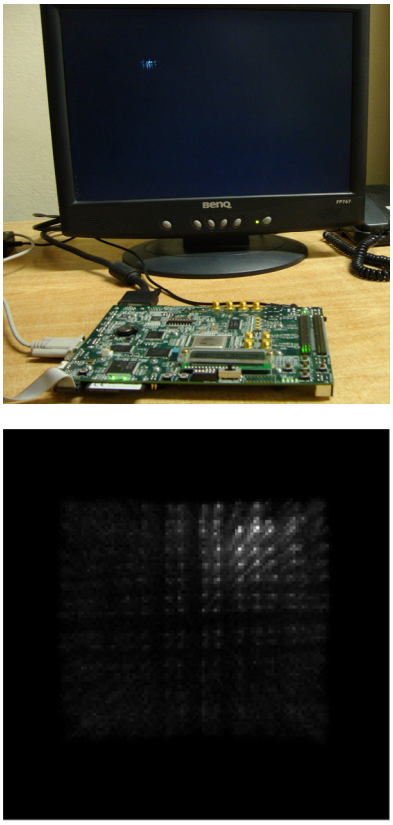

Fig. 17. Two dimensional output image obtained with the FPGA in a VGA monitor

Element	Specification
FPGA technology	90nm triple-oxide process
Number of Block RAMs	3
Number of Slices	53
Number 4 input LUTs	89
Clock frequency	322 MHz
Area Occupancy	25%

Table 2. Technical data for the FPGA architecture

6. Conclusions and future work

In this paper the implementation of a read out electronics prototype for a gamma camera has been presented. The system has successfully included reprogrammable devices in order to accelerate a two-dimensional image construction. A board containing a Virtex IV FPGA was used for implementation where parallel techniques and an efficient management of data and a reduced access to memory were used. The obtained system provides enough flexibility for adjustment to new requirements or new algorithms. The main contribution of this work consists on validating the use of a FPGA in the image processing stage for a nuclear medicine application.

Nowadays this application is being developed looking for the reconstruction to be performed in real time. Based on results obtained for planar images; as future work it is proposed the implementation of the filtered back projection algorithm for image reconstruction inside the FPGA in order to accelerate it.

Even though ^{137}Cs is not the most commonly source used in a gamma camera, in the present work it was employed due to as future work it is planned to extend the prototype to the implementation of a PET system.

7. References

Anger, Hal O. (1958). Scintillation Camera, *Review of scientific instruments*, Vol.29, No.1, (January 1958), pp. 27-33, ISSN 0034-6748.

Simon R., et al. (2003). *Physics in Nuclear Medicine*, Elsevier, ISBN 9780721683416, Philadelphia, USA.

Sánchez, F., Et al. (2004). Design and tests of a portable mini gamma camera, *Medical Physics*, Vol.31, No.6, (May 2004), pp. 1384-1396, ISSN 0094-2405.

Zhang, N., et al. (2002). Anode Position and Last Dynode Timing Circuits for Dual-Layer BGO Scintillator With PS-PMT Based Modular PET Detectors, *IEEE Transactions on Nuclear Science*, Vol.49, No.5, (October 2002), pp. 2203-2207, DOI: 10.1109/TNS.2002.803815

Demetri, P. & Jonathon A. (2005). Compact Readout Electronics for Position Sensitive Photomultiplier Tubes, *IEEE Transactions on Nuclear Science*, Vol.52, No.1, (February 2005), pp. 21-27, DOI: 10.1109/TNS.2004.843134

Hamamatsu Photonics, Electron Tube Center, H8500 Data Sheet (2007).

Chen, J., et al. (2007). Gamma-Ray Induced Radiation Damage in Large Size LSO and LYSO Crystal Samples, *IEEE Transactions in Nuclear Science*, Vol.54, No.4, (August 2007), pp. 1319-1326, ISSN 9781-4244-3962-1.

Olcott, P. D., et al. (2006). Compact Readout Electronics for Position Sensitive Photomultiplier Tubes, *IEEE Transactions in Nuclear Science*, Vol.53, No.5, (October 2006), pp. 2698-2703, ISSN .

Wong, W. (2006). A High Count Rate Position Decoding and Energy Measuring Method for Nuclear Cameras Using Anger Logic Detectors, *IEEE Transactions in Nuclear Science*, Vol.45, No.3, (June 2006), pp. 1122-1127, ISSN.

Knoll, G. F. (2000). *Radiation detection and measurement*, John Wiley, ISBN 978-0-471-07338-3,Michigan, USA.